

15 May 2004

The Influence of Strontium Substitution in Fluorapatite Glasses and Glass-Ceramics

R. G. Hill


A. Stamboulis

R. V. Law

A. Clifford

et. al. For a complete list of authors, see https://scholarsmine.mst.edu/che_bioeng_facwork/1222

Follow this and additional works at: https://scholarsmine.mst.edu/che_bioeng_facwork

 Part of the [Biochemical and Biomolecular Engineering Commons](#), and the [Biomedical Devices and Instrumentation Commons](#)

Recommended Citation

R. G. Hill et al., "The Influence of Strontium Substitution in Fluorapatite Glasses and Glass-Ceramics," *Journal of Non-Crystalline Solids*, vol. 336, no. 3, pp. 223 - 229, Elsevier, May 2004.

The definitive version is available at <https://doi.org/10.1016/j.jnoncrysol.2004.02.005>

This Article - Journal is brought to you for free and open access by Scholars' Mine. It has been accepted for inclusion in Chemical and Biochemical Engineering Faculty Research & Creative Works by an authorized administrator of Scholars' Mine. This work is protected by U. S. Copyright Law. Unauthorized use including reproduction for redistribution requires the permission of the copyright holder. For more information, please contact scholarsmine@mst.edu.

The influence of strontium substitution in fluorapatite glasses and glass-ceramics

R.G. Hill ^{a,*}, A. Stamboulis ^a, R.V. Law ^b, A. Clifford ^c, M.R. Towler ^c, C. Crowley ^d

^a Department of Materials, Imperial College London, South Kensington Campus, London SW7 2AZ, UK

^b Department of Chemistry, Imperial College London, South Kensington Campus, London SW7 2AZ, UK

^c Department of Materials, University of Limerick, Plassey, Limerick, Ireland

^d Materials Ireland Research Centre, Plassey Park, Limerick, Ireland

Received 19 March 2003

Abstract

Strontium is often substituted for calcium in order to confer radio-opacity in glasses used for dental cements, biocomposites and bioglass-ceramics. The present paper investigates the influence of substituting strontium for calcium in a glass of the following composition: $4.5\text{SiO}_2\text{3Al}_2\text{O}_3\text{1.5P}_2\text{O}_5\text{3CaO2CaF}_2$, having a Ca:P ratio of 1.67 corresponding to calcium fluorapatite ($\text{Ca}_5(\text{PO}_4)_3\text{F}$). The glasses were characterized by magic angle spinning nuclear magnetic resonance (MAS-NMR), by differential scanning calorimetry (DSC) and X-ray powder diffraction (XRD). The ^{29}Si , ^{27}Al and ^{31}P NMR spectra for the glasses with different strontium contents were identical. The ^{19}F spectra indicated the presence of F–Ca(n) and Al–F–Ca(n) species in the calcium glasses and in the strontium glasses F–Sr(n) and Al–F–Sr(n). It can be concluded that strontium substitutes for calcium with little change in the glass structure as a result of their similar charge to size ratio. The low strontium glasses bulk nucleated to a calcium apatite phase. Intermediate strontium content glasses surface nucleated to a mixed calcium–strontium apatite and the fully strontium substituted glass to strontium fluorapatite.

© 2004 Elsevier B.V. All rights reserved.

1. Introduction

Calcium fluoro-alumino-silicate glasses are used for the formation of polyalkenoate cements used for medical and dental applications. Commercial compositions also contain phosphate and strontium. Strontium is substituted for calcium to give the cements radio-opacity. Recently Hill and co-workers [1–6] and Höland and co-workers [7–9] have shown that such glasses can crystallize to fluorapatite. Fluorapatite glass-ceramics are attractive materials for medical and dental applications, since apatite is the mineral phase of tooth and bone. Hydroxyapatite (HA) based materials are generally produced by a sintering route. However there are considerable problems encountered on sintering HA, notably arising from its degradation at high temperatures [10,11]. All the sintered HA materials lack suffi-

cient strength and toughness. Furthermore sintering is not an attractive route for the production of the complex shapes required for substitute bone parts, dental crowns and inlays. Subsequent machining using diamond tipped tools is required to form the intricate shapes needed. Such machining is time consuming and expensive. Glass-ceramics are an attractive production route for producing apatite based materials offering the ability to cast components in the glassy state, directly to the required shape. Near net shapes can be produced and the technique is suitable for the production of ‘one off’ shapes. However, the most extensively studied glass-ceramic for potential use as a bone substitute material is the apatite–wollastonite, AW, system which cannot be cast to shape and is processed by a sintering route [12].

Hill and co-workers [1–6] developed a readily castable fluorapatite glass-ceramic from the $\text{SiO}_2\text{–Al}_2\text{O}_3\text{–P}_2\text{O}_5\text{–CaO–CaF}_2$ system from research undertaken on ionomer glasses used in glass (ionomer) polyalkenoate cements. The high fluorite content glasses of this system were shown to crystallize to fluorapatite and mullite and exhibited bulk nucleation, via prior amorphous phase

* Corresponding author. Tel.: +44-20 7594 6783; fax: +44-20 7584 3194.

E-mail address: r.hill@ic.ac.uk (R.G. Hill).

separation [2]. Dimitrova-Lukacs and Gillemot [13] have demonstrated that one of the compositions studied by Hill et al. [1], when cerammed, gives a material with high fracture toughness (2.7 MPa \sqrt{m}) and high strength (>260 MPa). Subsequently Clifford et al. [3] confirmed that high fracture toughness values could be obtained. The high fracture toughness is thought to arise from the microstructure, which consists of interlocking apatite and mullite crystals. The apatite crystals can have an aspect ratio greater than 50 and during fracture these needle like crystals are pulled out giving rise to high fracture toughness values.

For some medical and dental applications, glasses that are opaque to X-rays are required. The glasses and glass-ceramics developed to date lack sufficient radio-opacity. The present study investigates the substitution of strontium for calcium on the nucleation and crystallization behavior of one previously studied composition [4,6] that has a Ca:P ratio of 1.67 corresponding to apatite and crystallizes to calcium fluorapatite. Strontium has an ionic radius of 1.16 nm, close to that of calcium at 0.94 nm and therefore strontium may be substituted in these glass compositions for calcium. Strontium not only substitutes for calcium in glasses, but may also be substituted in crystalline structures. Of most interest is the substitution of strontium in apatite structures. Solid solutions of strontium–calcium hydroxyapatite (Sr,Ca)₁₀(PO₄)₆(OH)₂, and pure strontium apatite are reported in the mineral form and have been produced from aqueous solutions [14]. Introduction of strontium into the apatite lattice results in an increase in the unit cell dimensions, with *a* and *c* increasing to 0.976 and 0.728 nm respectively compared to 0.942, 0.688 nm for HA. This increase is associated with the slightly larger ionic radius for strontium. The change in cell dimensions produces an X-ray diffraction pattern for strontium apatite with larger *d*-spacings than its calcium counterpart. The increased atomic weight and number of strontium results in increased density of both the glass and crystal structure, and will produce a material with increased X-ray radio-opacity. The ability to observe a materials location and behavior in service is a crucial feature for materials for both medical and dental applications.

The present paper investigates the influence of substituting Sr for Ca on the structure of an apatite

stoichiometry glass and its influence on the nucleation and crystallization behavior. The glass studied is from a series of glasses based on: 4.5SiO₂3Al₂O₃1.5P₂O₅–*z*CaO*z*CaF₂ which have been the subject of a number of previous studies [4,15,16] including characterization by ²⁹Si, ²⁷Al and ³¹P and ¹⁹F MAS-NMR [15,16].

2. Experimental

2.1. Glass design

A previously studied glass with the composition 4.5SiO₂3Al₂O₃1.5P₂O₅3CaO2CaF₂ was selected for this work. This glass has an excess fluorine content compared to the fluorapatite stoichiometry. Strontium was substituted for calcium on a molar basis. Firstly SrO was substituted for CaO and then SrF₂ for CaF₂. The glass compositions produced are given in Table 1.

All the glass compositions studied contain sufficient phosphorus and calcium according to Lowenstein's rules [17] to allow the aluminum to take up Al(IV). Other criteria included ensuring the presence of at least one non-bridging oxygen (NBO) per silicon, maintaining Al³⁺ in a fourfold co-ordination state and ensuring fluorine content was less than the aluminum content in order to minimize silicon tetrafluoride, SiF₄ volatilization during melting. These criteria are based on the fact that an Si⁴⁺ cation will have a higher affinity for a NBO, or O²⁻ anion, than for a non-bridging fluorine or F⁻ anion and that an Al³⁺ ion will bond the F⁻ anion, so preventing the formation of Si–F bonds in the glass network. The model is supported by a trimethylsilylation analysis [18] of a previously studied 2SiO₂Al₂O₃CaO–CaF₂ glass, which demonstrated the absence of Si–F bonds.

3. Experimental

3.1. Glass synthesis

The glasses were produced by melting the reagents, silica, alumina, phosphorus pentoxide, calcium carbonate, calcium fluoride, strontium carbonate and strontium fluoride in the required amounts in high density

Table 1
Composition of the glasses studied

Glass code	SiO ₂	Al ₂ O ₃	P ₂ O ₅	CaO	CaF ₂	SrO	SrF ₂
LG26	4.5	3	1.5	3	2	0	0
LG119	4.5	3	1.5	1.5	2	1.5	0
LG125	4.5	3	1.5	0	2	3	0
LG26Sr	4.5	3	1.5	0	0	3	2

mullite crucibles (Zedmark Refractories Earlsheaton Dewsbury, UK) at a temperature of 1420 °C for 2 h. The resulting melts were rapidly shock quenched into water to prevent phase separation and crystallization. The glass frit produced was ground and sieved to give fine (<45 µm) and coarse (45–200 µm) particles, which were used in the subsequent analysis.

3.2. Glass characterization

3.2.1. MAS-NMR

MAS-NMR analyses were conducted on ^{29}Si , ^{27}Al , ^{31}P and ^{19}F nuclei at resonance frequencies of 39.77, 52.15, 81.01 and 188.29 MHz, respectively, using an FT-NMR spectrometer (AM-200, Bruker, Germany). Spinning rates of the samples at the magic angle were 5 kHz for the ^{29}Si , ^{27}Al , ^{31}P MAS-NMR and 15 kHz for ^{19}F . Recycle time was 2 s for ^{29}Si , ^{27}Al , and 4s for ^{31}P and 120s for ^{19}F . Reference materials for the chemical shift (in ppm) were tetramethylsilane for ^{29}Si , yttrium aluminum garnite (YAG) for ^{27}Al , 85% H_3PO_4 for ^{31}P and their chemical shift was adjusted to zero ppm. The spectra for ^{19}F were referenced to CaF_2 taken as -108 ppm relative to the more common standard of CFCl_3 .

3.2.2. Differential scanning calorimetry (DSC)

The glasses produced were characterized by differential scanning calorimetry using a Stanton Redcroft DSC 1500 (Rheometric Scientific, Epsom, UK). The crucibles used were matched pairs made of a platinum–rhodium alloy. Alumina was used as the reference material. Runs were performed in dry nitrogen at a heating rate of 10 °C min^{-1} . The tendency of the glasses to undergo surface nucleation was assessed by performing DSC runs using two particle sizes; frit particles of 1–2 mm and fine of <45 µm.

3.2.3. X-ray powder diffraction

X-ray powder diffraction analysis was completed on heat-treated glass samples for qualitative purposes. A Philips powder diffractometer (Philips Xpert diffractometer, Philips Eindhoven, NL) was used with Cu K_α X-rays. Every glass composition was heat treated using the tube furnace of the DSC to replicate the DSC analysis using an identical heating rate with samples taken at the individual crystallization temperatures for each glass.

4. Results and discussion

4.1. MAS-NMR spectra

4.1.1. ^{29}Si MAS-NMR spectra

Fig. 1 shows ^{29}Si MAS-NMR spectrum of the original LG26 glass. The silicon spectra show a large broad

peak at -90 ppm that was independent of the strontium content. The chemical shift observed for Si in a four coordinate state is between -60 and -100 ppm. Engelhardt et al. [19] ascertained that the chemical shift of Si in calcium alumino-silicate glasses depended on both the number of bridging oxygen (m) per SiO_4 unit and the number of aluminum (n) connected by oxygen with the SiO_4 unit. When a structural unit of the alumino-silicate glass network is expressed as $\text{Si}(\text{OSi})_{m-n}(\text{OAl}^-)_n(\text{O}^-)_{4-m}$, ($\text{Q}^m(n\text{Al})$, $4 \geq m \geq n \geq 0$), the chemical shift increases with decreasing m or increasing n . The chemical shift observed is in the region expected for Si in $\text{Q}^4(4\text{Al})$ and $\text{Q}^3(3\text{Al})$ environments.

4.1.2. ^{27}Al MAS-NMR spectra

Fig. 1 shows ^{27}Al MAS-NMR spectrum of the LG26 glass. The spectrum shows a characteristic broad resonance around 50 ppm that was again independent of strontium content. The chemical shift value is in the range for aluminum in a Al(IV) state, but is low compared with that of pure alumino-silicate glasses [19]. It has been reported that the chemical shift of Al decreased with SiO_2 content in the calcium alumino-silicate glasses of various $\text{CaO}/\text{Al}_2\text{O}_3$ ratios [19–21]. The chemical shift observed in the Al spectra (50 ppm) is lower by about 10 ppm than in a calcium alumino-silicate glass (60 ppm) containing no P_2O_5 based on anorthite [22]. The difference in chemical shift is probably due to the presence of P_2O_5 . P_2O_5 exists as PO_4 tetrahedra in the glass, some of which are probably connected with AlO_4 tetrahedra. The P^{5+} ion will locally charge compensate for the charge deficient Al^{3+} ion. P atoms are more electronegative than Si atoms and the Al–O–P bond formation causes the negative shift observed in the ^{27}Al MAS-NMR spectrum.

The spectra of the strontium-substituted glass (LG26Sr) are identical to the LG26 composition. The substitution of Sr for Ca therefore does not influence the ^{27}Al spectrum of the glass.

4.1.3. ^{31}P MAS-NMR spectra

Fig. 1 shows the ^{31}P MAS-NMR spectrum of the LG26 glass. There was again no change in the spectra with increasing strontium content. A large symmetrical broad peak was observed around -5 ppm together with two side bands around 28 and -40 ppm. The chemical shift of AlPO_4 (Q^4) is at -29 ppm [23] and that for orthophosphate (Q^0) at about 2–3 ppm [24] and pyrophosphate (Q^1) at between -4 and -20 ppm [23]. The peak at -5 ppm is attributed to a pyrophosphate type environment. The presence of strontium does not affect the chemical environment of P in the glasses. The Al ions most likely form Al–O–P linkages and thus it can be assumed AlPO_4^{3-} (Q^1) type species are probably present.

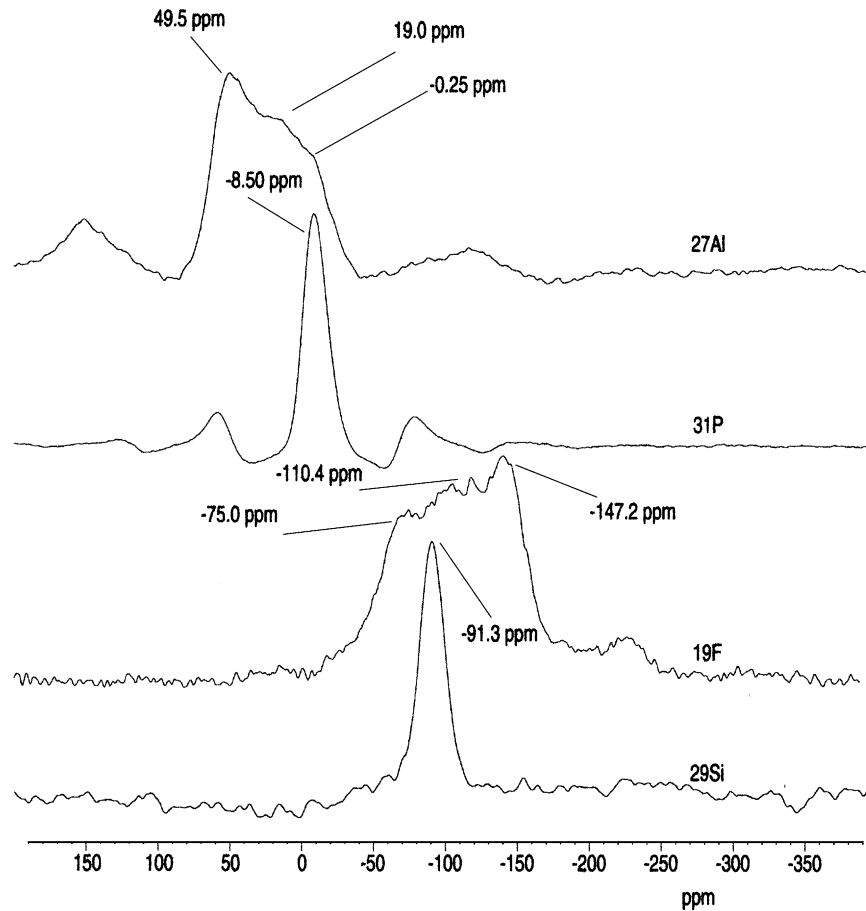


Fig. 1. ^{29}Si , ^{27}Al and ^{31}P MAS-NMR spectra for the LG26 glass.

4.1.4. ^{19}F MAS-NMR spectra

The probe backgrounds was quite large and therefore the background was subtracted after carefully measuring a sample free probe. The spectra were referenced to CaF_2 taken as -108 ppm relative to the more common standard of CFCl_3 . Fig. 2 shows the chemical shifts of the glasses for ^{19}F . In order to verify the ^{19}F spectra (as the background that needed to be subtracted was considerable) experiments on specially heat-treated samples

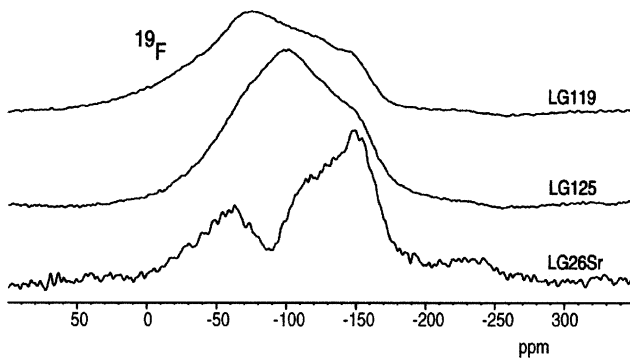


Fig. 2. ^{19}F MAS-NMR spectra for the glasses of different strontium content.

of the LG26 glass were run. It was expected that the glasses would crystallize to fluorapatite, something that was obvious from the ^{19}F spectra (Fig. 3) that showed a sharp peak at around -103 ppm, which is the one

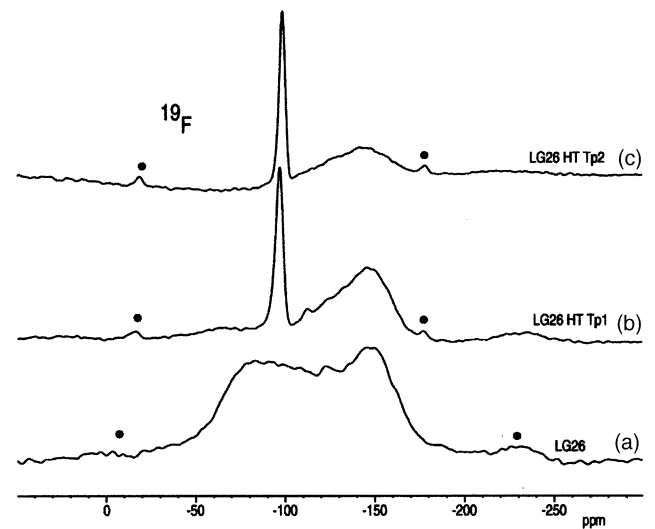


Fig. 3. ^{19}F MAS-NMR spectra of the LG26 glass (a) and the LG26 glass heat treated to T_{p1} (b) and T_{p2} (c).

associated with the crystalline phase of fluorapatite [25]. A second broad peak at around -150 ppm suggested the presence of the fluorine in the amorphous glass phase, which according to Zeng and Stebbins [26] and Stebbins and Zeng [27] is attributed to a Al–F–Ca(n) species.

Fig. 2 shows the ^{19}F MAS-NMR spectra. The LG26 glass exhibited one broad peak at ca. -100 ppm and one smaller peak at ca. -150 ppm. The first is associated with a F–Ca(n) environment, whereas the second peak is associated with Al–F–Ca(n) environment [26,27]. Substituting Sr for Ca in the LG26 glass results in a very slight shift in the spectra and indicates the presence of F–Sr(n) and Al–F–Sr(n). The peak at -100 ppm shifts to less negative values on strontium substitution and is attributed to F–Sr(n), whilst the peak at -150 ppm is attributed to Al–F–Sr(n).

In conclusion, substituting strontium for calcium has very little influence on the structure of the glass and this is probably a result of the identical charge of the ions and their similar size.

4.2. Crystallization behavior

4.2.1. Differential scanning calorimetry

Differential scanning calorimetry was completed on two particles sizes for each glass (<45 μm , frit), and the results are given in Table 2. The glass transition temperature (T_g) decreased slightly with increasing substitution of strontium for calcium initially then rises slightly. The largest decrease was approximately 34 $^\circ\text{C}$ for LG125 (3SrO), this change is considered significant. The decrease in glass transition temperature is associated with the increased disruption to the glass network by the slightly larger strontium cation, and the weaker strontium–oxygen bond strength. The increase in the T_g of the fully strontium substituted glass is difficult to explain.

The first crystallization temperature (T_{p1}) which corresponded to fluorapatite in the calcium glass depended on particle size and strontium substitution. The LG26 (0SrO) exhibited complete bulk nucleation with the first crystallization temperature being independent of particle size, increasing the strontium content results in altering the mechanisms for nucleation. Complete substitution of strontium oxide for calcium produces a glass composition, which exhibits predominantly surface

nucleation. The initial substitution of strontium into the glass structure reduces the values obtained for the first peak crystallization temperature slightly and the glass still bulk nucleates. Higher strontium substitutions appear to hinder the crystallization of apatite, which is reflected in an increase in crystallization temperature, and promotion of surface nucleation of apatite at the expense of bulk nucleation, as evidenced by the increase in the first crystallization temperature (T_{p1}) with particle size.

The second crystallization process (T_{p2}) is also influenced by the substitution of strontium in the glass structure. Initial substitution (1.5SrO) of strontium reduces T_{p2} by 15 $^\circ\text{C}$, an effect associated with the increased mobility of the network and its lower T_g , and also introduces a more dominant surface effect. Complete substitution of strontium oxide for calcium oxide reduces the T_{p2} value considerably, from 930 to 805 $^\circ\text{C}$ for the <45 μm material, and also promotes surface nucleation. Such a reduction in crystallization temperature would suggest a new crystalline phase, and not simply a reduction in crystallization temperature.

In the fully strontium substituted glass LG26Sr T_{p2} disappears for the <45 μm glass particle size but is still present for the frit samples.

4.2.2. X-ray diffraction analysis

X-ray powder diffraction analysis was completed on heat-treated samples of each glass. LG26 and LG119 (SrO = 0, 1.5 respectively) were both shown to crystallized to calcium fluorapatite and mullite on heat treatment up to their respective second peak crystallization temperatures ($T_{p2} = 931$ and 915 $^\circ\text{C}$ respectively). The X-ray diffraction pattern for both glasses corresponded with the pattern for FAP. It is thought that no solid solutions are formed under these conditions. Quantitative analysis was not completed on these materials but X-ray diffraction line intensities are very similar for both LG26 and LG119, indicating no depletion in the quantity of fluorapatite formed. It is noted however that the overall degree of crystallinity is low, given the relatively large amorphous region on the traces. Given no evidence for strontium in the crystalline apatite lattice, then it is assumed to remain within the glassy network as network modifying cations or network dwelling cations locally charge balancing the aluminum cations.

Table 2
DSC analysis data

Glass	SrO + SrF ₂	T_g ($^\circ\text{C}$)	T_{p1} ($^\circ\text{C}$)		T_{p2} ($^\circ\text{C}$)	
			<45 μm	Frit	<45 μm	Frit
LG26	0	640	740	740	930	931
LG119	1.5	616	737	734	915	888
LG125	3	606	757	779	805	815
LG26Sr	5	649	814	875	nd	968

LG125 having complete substitution of CaO for SrO was shown to undergo surface nucleation for both the first and second crystallization processes. X-ray powder analysis of LG125 heat treated to 800 °C gave neither a pure fluorapatite nor a strontium apatite as the crystalline phase. The diffraction pattern produced by this sample was similar to that of calcium fluorapatite, but the pattern was shifted to higher d -spacings (lower 2θ angles). Shifting the diffraction lines to higher d -spacings and broadening the peaks suggests a solid solution of strontium/calcium apatite is forming. According to Vegard's law, unit cell parameters should change linearly with compositions. In practice this law is only approximated and is more problematic for non-cubic systems. However, application of Vegard's law to this glass-ceramic gives an approximate degree of solid solution to be 55% calcium.

High concentrations of strontium therefore result in the formation of a solid solution of calcium/strontium fluorapatite. However, differential scanning calorimetry showed this phase to surface nucleate unlike the bulk nucleating calcium fluorapatite. The change in mechanism for nucleation may be possibly associated with the increased size of the strontium cation compared to calcium. Given that fluorine slightly reduces the lattice parameters of apatite with an associated lowering of its lattice energy then the inclusion of a large strontium cation would be unfavorable. Alternatively strontium may also be inhibiting the amorphous phase separation process that has been shown to occur prior to crystal nucleation in the LG26 composition [28] and is thought to give rise to the observed internal bulk crystal nucleation.

The completely strontium substituted glass LG26Sr crystallized to strontium fluorapatite at T_{p1} . A typical XRD pattern is shown in Fig. 4. The presence of

strontium fluorapatite was confirmed using ^{19}F and ^{31}P MAS-NMR spectroscopy of the heat-treated glass. Fig. 5 shows the ^{19}F spectrum. The ^{19}F spectrum shows a sharp peak at about -64 ppm corresponding to strontium fluorapatite and the ^{31}P spectra has a sharp peak with a chemical shift at 2–3 ppm characteristic of an orthophosphate.

The crystal phase corresponding to T_{p2} in the LG125 glass was determined to be surface nucleating anorthite ($\text{CaSi}_2\text{Al}_2\text{O}_8$) and not mullite. The presence of anorthite and not mullite in these glass-ceramics has been reported previously [4]. The crystallization of anorthite is a result in the reduction in quantity of apatite produced by the system, leaving increased quantities of calcium within the glass network, and this subsequently forms anorthite.

The crystal phase corresponding to T_{p2} in the full strontium substituted glass LG26Sr exhibited a single very pronounced diffraction line at about $7.5^\circ 2\theta$. It did

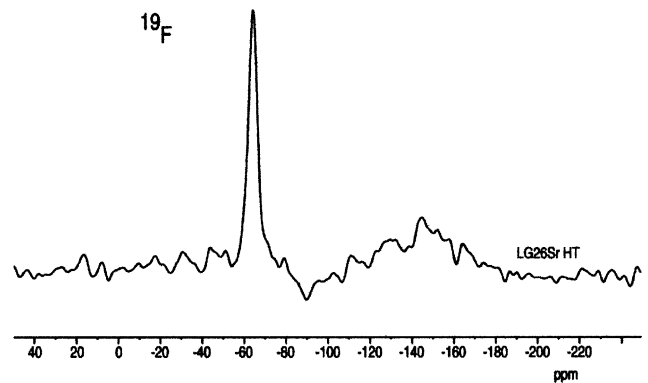


Fig. 5. ^{19}F MAS-NMR spectra of LG26Sr heat treated to T_{p1} .

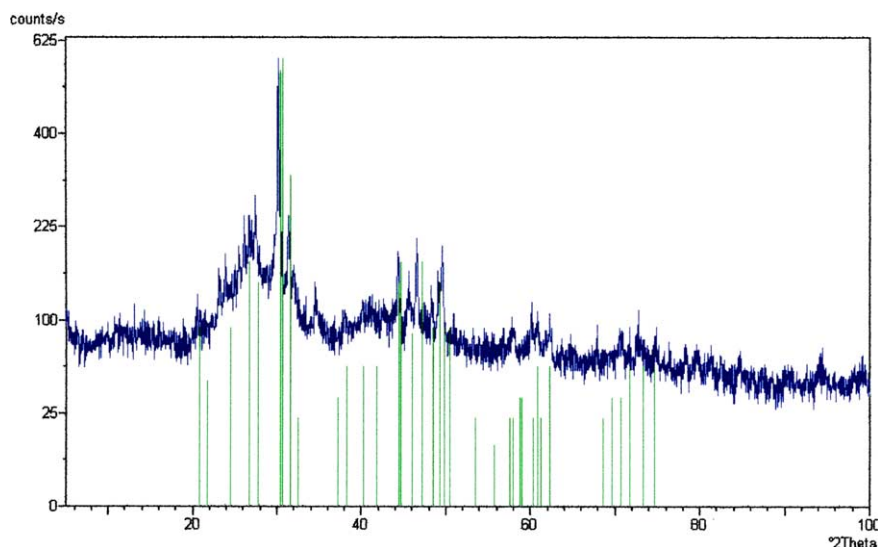


Fig. 4. XRD pattern of the LG26Sr glass heat treated to T_{p1} showing a match to $\text{Sr}_5(\text{PO}_4)_3\text{F}$.

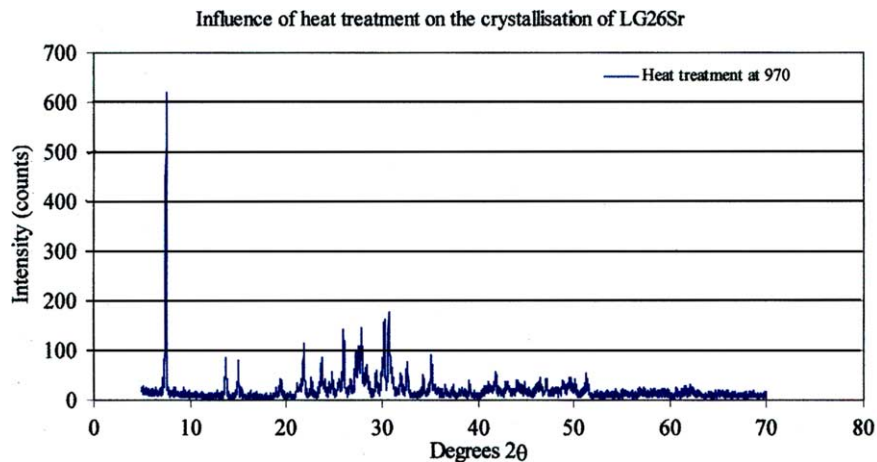


Fig. 6. XRD pattern of LG26Sr heat treated at T_{p2} . Note the sharp diffraction line corresponding to an unknown phase at $7.5^\circ 2\theta$.

not correspond to either mullite or anorthite and has not yet been identified (Fig. 6).

5. Conclusions

Substituting strontium for calcium has little influence on the glass structure with strontium replacing F–Ca(n) by F–Sr(n) and Al–F–Ca(n) by Al–F–Sr(n). Strontium substitution for calcium does however influence the nucleation and crystallization behavior of the glass. Replacement of calcium by strontium promotes surface nucleation of the apatite phase. Low strontium substitutions result in a calcium fluorapatite phase being formed first, higher strontium substitutions result in a mixed calcium/strontium fluorapatite being formed. Complete strontium substitution results in strontium fluorapatite crystallizing. The fact that strontium hinders apatite phase formation and inhibits bulk nucleation may be a result of two factors: the lower lattice energy of strontium fluorapatite and possibly strontium suppressing the amorphous phase separation that is known to occur in the strontium free glass.

References

- [1] R.G. Hill, M. Patel, D.J. Wood, in: W. Bonfield, G.W. Hastings, K.E. Tanner (Eds.), *Bioceramics*, vol. 4, Butterworth–Heinmann, London, 1991, p. 79.
- [2] R. Hill, D. Wood, *J. Mater. Sci. Mater. Med.* 6 (1995) 311.
- [3] A. Clifford, R. Hill, *J. Non-Cryst. Solids* 196 (1996) 346.
- [4] A. Rafferty, A. Clifford, R. Hill, D. Wood, B. Samuneva, M. Dimitrova-Lukacs, *J. Am. Ceram. Soc.* 83 (2000) 2833.
- [5] A. Clifford, R. Hill, A. Rafferty, P. Mooney, D. Wood, B. Samuneva, S. Matusuya, *J. Mater. Sci. Mater. Med.* 12 (2001) 461.
- [6] K. Stanton, R. Hill, *J. Mater. Sci.* 35 (2000) 1911.
- [7] C. Jana, W. Höland, *Silic. Ind.* 56 (1991) 215.
- [8] I. Szabó, B. Nagy, G. Völksch, W. Höland, *J. Non-Cryst. Solids* 212 (2000) 191.
- [9] W. Höland, V. Rheinberger, M. Frank, *J. Non-Cryst. Solids* 253 (1999) 170.
- [10] W.R. Rao, R.F. Boehm, *J. Dent. Res.* (1973) 1351.
- [11] H.A.M. Jarch, C.H. Bolen, M.B. Thomas, J. Bobick, J.F. Kay, R.H. Doremus, *J. Mater. Sci.* (1976) 2027.
- [12] T. Kokubo, S. Ito, S. Sakka, *J. Mater. Sci.* 21 (1986) 535.
- [13] M. Dimitrova-Lukacs, L. Gillemot, in: P. Duran, J.F. Fernandez Faenza (Eds.), *Third Euroceramics*, Vol. 3, Editrice Iberica S.L., Spain, 1993, p. 179.
- [14] F.C.M. Driessens, R.M.H. Veerbeek, *Biomaterials*, CRC, 1990.
- [15] S. Matusuya, A. Stamboulis, R. Hill, R.V. Law, in preparation.
- [16] R. Hill, A. Stamboulis, R.V. Law, S. Matusuya, A MAS-NMR study of the crystallisation process of apatite–mullite glass-ceramics, *J. Phys. Chem. Glasses*, in press.
- [17] W. Lowenstein, *Am. Mineral.* 39 (1954) 92.
- [18] R. Hill, D. Wood, M. Thomas, *J. Mater. Sci.* 34 (1999) 1767.
- [19] G. Engelhardt, M. Noftz, K. Forkel, F.G. Wishmann, M. Magi, A. Samson, E. Lippma, *Phys. Chem. Glasses* 26 (1985) 157.
- [20] M. Schmucker, K.J.D. Mackenzie, H. Schneider, R. Meinhold, *J. Non-Cryst. Solids* 217 (1997) 105.
- [21] E.D. Lacy, *Phys. Chem. Glasses* 4 (1963) 234.
- [22] A. Stamboulis, R. Hill, R.V. Law, *J. Non-Cryst. Solids* 333 (2004) 101.
- [23] W.A. Dollase, L.H. Merwin, A. Sebald, *J. Solid State Chem.* 83 (1989) 140.
- [24] R. Dupree, D. Holland, M.G. Mortuza, J.A. Collins, M.W.G. Lockyer, *J. Non-Cryst. Solids* 112 (1989) 111.
- [25] M. Braun, C. Jana, *Chem. Phys. Lett.* 245 (1995) 19.
- [26] Q. Zeng, J.F. Stebbins, *Am. Mineral.* 85 (2000) 863.
- [27] J.F. Stebbins, Q. Zeng, *J. Non-Cryst. Solids* 262 (2000) 1.
- [28] A. Rafferty, R. Hill, D. Wood, *J. Mater. Sci.* 35 (2000) 3863.